Chlamydomonas reinhardtii displays aversive swimming response to silver nanoparticles

MICHAEL R. MITZEL[1,2] NICHOLAS LIN[1], JOANN K. WHALEN[2] and NATHALIE TUFENKJI[1*]

[1]Department of Chemical Engineering,
[2]Department of Natural Resource Sciences,
McGill University, Montreal, Quebec H3A 0C5, Canada

[*] *Corresponding Author. Phone: (514) 398-2999; Fax: (514) 398-6678; E-mail: nathalie.tufenkji@mcgill.ca*

Abstract

Engineered nanoparticles (ENPs) present in the environment are a potential risk to soil health, water safety and human health. Physical responses of microorganisms, such as avoidance behavior, could be an early indicator of biological outcomes upon exposure to ENP contamination. *Chlamydomonas reinhardtti* was exposed to gradients of nano-sized silver (*n*Ag; 50 nm), gold (*n*Au; 50 nm) and sulfated polystyrene latex (*n*SPL; 22 nm) in a microfluidics device. Videos captured at targeted locations using enhanced darkfield microscopy showed that *C. reinhardtii* moved away from areas containing *n*Ag at and above 6×10^{8} particles/mL. *C. reinhardtii* also avoided *n*SPL at and above 3×10^{10} particles/mL, but did not avoid *n*Au at 6×10^{8} or 6×10^{9} particles/mL. Dissolution of Ag^{+} around *n*Ag particles may elicit avoidance behavior by *C. reinhardtii*, as *C. reinhardtti* also responded to a gradient of Ag^{+} (at ≤ 1 μM). We conclude that *C. reinhardtii* respond when exposed to a toxicant, but they do not sense nanomaterials directly, given their inconsistent response to similar concentrations of *n*Ag, *n*SPL and *n*Au. Rather, we postulate that their greater sensitivity to *n*Ag than other ENPs is due to toxicity resulting from dissolved Ag^{+} around colloidal *n*Ag particles.

Keywords: Microfluidic; toxicology; engineered nanoparticles; environmental risk; algae;

Introduction

Silver nanoparticles (*n*Ag) are engineered nanoparticles (ENPs) found in numerous consumer products such as clothing, food storage containers, home appliances and sporting goods, [1-3] due to the potent and broad-spectrum antimicrobial activity of *n*Ag. Widespread use of *n*Ag in these and future consumer products will undoubtedly result in *n*Ag release into terrestrial and aquatic environments, where *n*Ag and Ag^+ will interact with indigenous biota.[4-6] The toxicity of *n*Ag to a variety of micro- and macro-organisms is known,[7-10] and mechanisms of *n*Ag toxicity include: damage to cell membranes or DNA, disruption of respiratory chains or gene expression, oxidative stress from reactive oxygen species production and ionic silver (Ag^+) release.[11-13] Ag^+ toxicity occurs through the same mechanisms, which created debate on whether the organismal responses to *n*Ag were the result of exposure to Ag^+ released by *n*Ag dissolution or a 'nano-specific' effect. An elegant study by Xiu et al.[14] ruled out nano-specific effects to *Escherichia coli* as no toxicity occurred under anaerobic conditions that prevented Ag^+ release.

Chlamydomonas reinhardtii is a unicellular, micron-sized, flagellated Chlorophyte present in a broad range of freshwater and soil[11] habitats and is well characterized (i.e., fully-sequenced genome).[15] Toxicity was reported for *C. reinhardtii* exposed to micromolar (μM) concentrations of *n*Ag with a variety of coatings,[16] although Ag^+ is more toxic to *C. reinhardtii* with toxicity observed at concentrations in the tens to hundreds of nanomolar (nM).[17-19] Previous studies of *C. reinhardtii* exposure to *n*Ag and Ag^+ were generally done in 'batch' experiments with exposure times of 1 hour or more, although Pillai et al.[20] investigated the molecular responses of *C. reinhardtii* to Ag^+ as soon as 15 min after exposure. In natural polluted environments where *C. reinhardtii* is found, heterogeneity is the norm, and toxicity studies conducted in a homogeneously contaminated experimental vessel would not account for this factor. Hence, an experimental design

that allows for heterogeneous exposure is of interest. If the motile *C. reinhardtii* is able to sense and avoid *n*Ag and other ENPs by swimming away, it will avoid the deleterious effects associated with these ENPs. Fundamental sensory-responses such as chemotaxis,[21,22] phototaxis,[23-25] and mechanotransduction[26] were elucidated with *C. reinhardtii*, but there is no work to date on whether this organism possesses a sensory detection system for ENPs.

This study aimed to determine whether individual *C. reinhardtii* swim away from *n*Ag, gold nanoparticles (*n*Au) and sulfated polystyrene latex nanoparticles (*n*SPL) during acute exposure (~30 s) to a curvilinear gradient of these ENPs. The movement of *C. reinhardtii* upon exposure to Ag^+ and algae growth medium was also investigated and compared to the ENP treatments. The swimming response of *C. reinhardtii* was evaluated using enhanced darkfield microscopy equipped with a CytoViva™ condenser designed for hyperspectral imaging, in combination with a microfluidic gradient generator coupled to an exposure chamber originally intended for bacterial chemotaxis studies,[27, 28] illustrated in Fig. 1. Due to the short timescale of each experiment and small pore volume (~280 nL) of the experimental system, no genetic or molecular information was collected. However, observing an organism's physical response, such as swimming-away (i.e., avoidance behavior), gives clues about the genetic and molecular machinery underlying the rapid, integrated cellular response (i.e., movement) in a motile unicellular organism, without the need for sample collection and processing.

Materials and Methods

Preparation and Characterization of Nanoparticle Suspensions

Econix™ polyvinylpyrrolidone-stabilized silver (PVP-*n*Ag) and Nanoexact™ PVP-stabilized gold nanoparticles (PVP-*n*Au) were purchased from Nanocomposix Inc. (San Diego, CA) as aqueous suspensions at a concentration of 5.2 mg/mL (5.8×10^{12} particles/mL) and 0.05 mg/mL (5.6×10^{10} particles/mL), respectively. Sulfate polystyrene latex 0.02 μm FluoSpheres® (*n*SPL) were purchased from Life Technologies (San Diego, CA) as a 2 % w/v (3.4×10^{15} particles/mL). Due to the difficulty in ensuring highly accurate nanoparticle concentrations following dilution, stock suspensions were prepared by serial dilution to ~ 6×10^n for nAg and *n*Au, and 3×10^n for *n*SPL. *n*SPL was included as an additional model non-ionic nanoparticle due to the unavailability of the commercial *n*Au at higher stock concentrations. Working suspensions of ENPs were prepared by dilution of the stock suspensions following bath sonication (Fisher Scientific FS140H, 42 ± 6 Hz) for 2 min before dilution in 1 mM $NaNO_3$ (pH 7.05) containing 0.1 mM MOPS buffer. The working suspension was then vortexed at maximum speed for 30 s to homogenize the diluted stock ENPs in the suspending buffer, prior to further dilution. Working ENP suspensions were prepared from their respective stocks 15 min prior to injection into the microfluidic device and experiments using these suspensions were completed within 2 h. The hydrodynamic diameters of ENPs were characterized within 15 min of preparing the working ENP suspension using dynamic light scattering (DLS; ZetaSizer Nano ZS, Malvern). Laser Doppler velocimetry in conjunction with phase analysis light scattering (Zetasizer Nano ZS) was also used to measure electrophoretic mobility (EPM) at 25 °C with an applied electrical field of 4.9 ± 0.1 V/m. EPMs were converted to ζ-potentials with the Henry equation using the Smoluchowski approximation. Multiple ionic strengths (IS) are examined in Supplementary Table S1 to illustrate ENP stability.

Dissolution of nAg

Ultracentrifugation and inductively-coupled plasma mass spectrometry (ICP-MS, Perkin Elmer) were used to determine the dissolution of *n*Ag suspended in 1 mM $NaNO_3$ solution. Ultracentrifugation was performed on suspensions of 6×10^7 through 10^{10} particles/mL following 2 h incubation. Exactly 6 mL of *n*Ag suspension was added to a thick-walled tube and centrifuged at 280,000×*g* for 15 min using a Sorvall mTX 150 Micro-Ultracentrifuge (ThermoFisher, Whitby, ON), then 5 mL of the supernatant was removed with a pipet, with care taken not to disturb the pellet in the remaining 1 mL. The procedure was repeated to obtain a total of 10 mL of supernatant, which was acidified with HNO_3 and digested at 85 °C for 500 min using DigiPREP digestion system. The digested samples were diluted to 3 % HNO_3 (v/v) before measurement with an ICP-MS. Quality control was performed with National Institute of Standards and Technology (NIST) standard solutions to verify the reliability of the ICP-MS analysis, blanks were included to correct for background signals, and the results are presented in Supplementary Fig. S1.

Growth and Preparation of Algae

Chlamydomonas reinhardtii stock culture was grown on agar plates with algae growth medium (hereafter referred to as algae medium) at 20 °C with 24 h light (~50 µmol/m^2 s) for one week and used as a source culture for up to 1 week. Two loopfuls of *C. reinhardtii* source culture were added to 40 mL of algae medium and grown for 48 h at 20 °C and 100 rpm with constant 24 h light from incandescent bulbs. The entire 40 mL was transferred into 200 mL of fresh algae medium and incubated for another 68 to 72 h at 20 °C and 100 rpm with constant light (~50 µmol/m^2s; incandescent). The algae medium recipe and culture protocols are provided in the *Supplementary Information*.

Next, 50 mL of *C. reinhardtii* culture was filtered using a 0.22 µm cellulose-acetate bottle top filter (Fisher Scientific, Whitby, ON) under low vacuum until a minimal amount of water remained on the surface of the filter (i.e., the algae residue was not allowed to dry). After turning off the vacuum, 5 mL of 1 mM $NaNO_3$ solution was added to the filter to re-suspend the algae residue using slight manual agitation. These re-suspended *C. reinhardtii* were then poured into a 15 mL Falcon tube (Fisher Scientific, Whitby, ON) and returned to the incubator for 15 min at 20 °C with light prior to use. Based on video observations, 36 ± 7 individual algae passed through the device inlet in each ~120 s video, which is equivalent to ~5.8 to 8.6 × 10^5 cells/mL.

Fabrication and Preparation of the Microfluidic Exposure Device

Microfluidic devices were created and prepared following the design of Englert et al.,[27, 28] with slight modifications. These modifications involved elongating the length of the channel from 11,500 µm to 15,400 µm, adding a ruler along one side of the channel marking 200 µm intervals, and designing the device to a total height of 2 mm. Soft-lithography silica molds and the resultant poly(dimethyl)siloxane (PDMS) devices were fabricated by Advanced Nano Design Applications (ANANDA, Montreal, QC). The PDMS-cast devices were plasma treated using a handheld plasma oxidizer (Electro-Technic Products Inc., Chicago, IL), dry baked at 60 °C for 20 min and primed with DI water. Additional materials needed for the preparation of microfluidic devices are provided in the Supplementary Information. See Englert et al. [28] for detailed microfluidic fabrication protocols.

Microfluidic Avoidance Experiments

Following assembly and flushing with DI water, the microfluidic device was transferred onto an Olympus BX51 polarizing microscope (10× UPlan, NA = 0.3) equipped with a CytoViva™ hyperspectral-enhanced darkfield condenser. One of two 2.5 mL glass syringes (Hamilton, ColeParmer, Montreal, QC) was filled with 1 mM $NaNO_3$ and the other was filled with 1 mM $NaNO_3$ supplemented with nanoparticles to a final concentration of: 6×10^8, 6×10^9 or 6×10^{10} PVP-*n*Ag/mL; 6×10^8 or 6×10^9 *n*Au/mL; and 3×10^9, 3×10^{10} or 3×10^{11} *n*SPL/mL. These concentrations provided similar specific surface areas (SSA) for the ENPs investigated (e.g., 6×10^8 *n*Au or *n*Ag and 3×10^9 *n*SPL correspond to 5×10^{-6} m^2/mL). Additional treatments examined were 1 and 10 µM $AgNO_3$ (in 1 mM $NaNO_3$), as well as algae medium alone. The ionic strength of 1 mM $NaNO_3$ solution selected for this study is 100-fold less than that of physiological saline solutions (approximately 150 to 300 mM; based on standard recipes),[30] but was necessary to avoid creating conditions that would cause ENPs to adhere to the microfluidic device. Syringes were mounted onto a programmable pump (KD Scientific, Model# 280036, Holliston, MA) positioned adjacent to the microscope and the device was flushed with the respective experimental solutions/suspensions for 5 min at 2.5 µL/min and 0.5 µL/min (for the gradient-maker inlets and the algae inlet, respectively). The flow rate was then reduced to 0.25 µL/min for the experimental solutions/suspensions and 0.05 µL/min for the algae, giving a total flow rate of 0.55 µL/min in the exposure channel. The device was then left to equilibrate for 20 min. Although the flow rate in this study was 4-fold lower (0.55 vs. 2.1 µL/min) than used by Englert et al.,[27, 28] this speed allowed the algae to swim freely, with characteristic pulses of 'run-and-tumble' motion toward the edges of the device. Under no- or low-flow conditions, *C. reinhardtii* swim with two coupled flagella pulling them forward in a breaststroke motion (see example video file in the Supplementary Information).[31] Under the moderate flow conditions used in this study, the algae appear to glide

and pulse, similar to the run-and-tumble motion in bacteria,[32] with the flagella uncoupled in order to turn more sharply (see link to example video in the Supplementary Information).[31] Faster flow rates interfered with observable pulses of swimming behavior and eliminated any run-and-tumble motion.

Algae swimming responses were acquired as 1920 × 1080 resolution videos, captured using a Samsung Galaxy Note4 smartphone (16 MP, f/2.2, 1.12 µm pixel size, default settings) that was mounted onto the ocular lens with the aid of a MiPlatform™ smartphone adaptor (Pro-Lab Diagnostics Inc., Richmond Hill, ON). Both top and bottom edges of the observation channel were kept in view and the focal area of the microscope maintained in the center of the microfluidic chamber. However, *C. reinhardtii* are photosensitive and to reduce the influence of light from the microscope on algae movement, the darkfield condenser was set deliberately out of focus, such that the light source illuminated the entire width of the microfluidic chamber. Once the equilibration process was completed, the microscope was placed on the 14,000 µm mark and left for 120 s. The camera was then moved to the 13,000 µm mark and this process continued, moving 1,000 µm until reaching the beginning of the channel (i.e., the algae inlet = 0 µm).

Analysis of Swimming Response

Videos were analyzed using Adobe® After Effects® CC Version 13.0.0.214 (San Jose, CA) to determine exact pixel locations of the algae. No image manipulation was performed. Approximately 30 to 50 individual *C. reinhardtti* cells were observed in each experiment and at each distance marking. Algae that were visibly stuck together, or that did not display evidence of pulsing flagella were excluded. Each treatment was investigated in quadruplicate microfluidic devices, resulting in observations about the position in the microfluidic chamber of at least 120

and less than 200 individual algae at each distance marking. Because of some uncontrolled factors, the number of algae observed in each 120 s video segment was unequal. Data was analyzed with linear regression analysis to determine the mean algae position (dependent variable) at each distance marking, for each of the 10 exposure treatments. Time was considered as a covariate through repeated measures analysis of variance in the preliminary analysis, but found to be insignificant ($F < 1$) in all cases. Linear regression analysis was performed using the mean of the frequency distribution generated at each distance marking to generate the slope of the line describing the swimming tendency of *C. reinhardtti* through the device (i.e., deviation from the centerline of the device). Slopes were analyzed to determine if they differed significantly from 0 ($\alpha = 0.05$). The slope of the regression line was also converted to an angle of deviation using a Pythagorean trigonometric identity.

Results

C. reinhardtii swimming behaviour in algae medium

The microfluidics device was equipped with two inlets, one for the background buffer solution (1 mM $NaNO_3$), and the other for ENPs suspended in buffer solution, which created a model heterogeneously contaminated environment in the exposure chamber because of the gradient generator. This would permit *C. reinhardtti* to swim away from the ENP-laden regions, down the gradient and into the buffer solution, if they could adapt their swimming direction to avoid contact with ENPs. The slope of the regression line based on the average location at each 1000 µm distance marking (Fig. S2 through Fig. S5 and Table S2) was used to calculate an angle of deviation (from the centerline of the device) for their movement and represented in Fig. 2 through Fig. 5 with a directional arrow. In a control experiment, *C. reinhardtti* was exposed to algae medium versus

buffer solution, assuming that algae would produce an observable positive response (i.e., would swim toward the medium). The swimming direction of *C. reinhardtti* did not exhibit a significant directional shift from zero ($F_{1, 13} = 4.24$, $p = 0.06$, Fig. 2a), although this result is very close to the $p = 0.05$ significance threshold. Overall, these results indicate that *C. reinhardtti* were equally likely to swim in the algae medium or buffer solution when no ENPs were present. Experiments conducted with buffer solution (1 mM $NaNO_3$) in both inlets produced no significant change in slope from zero ($F_{1, 13} = 0.15$, p = n.a; Supplementary Fig. S6).

Algae significantly avoid ionic Ag at 1 µ*M, but not 10* µ*M*

We posited that *C. reinhardtii* could be changing their swimming direction in response to chemical properties of the *n*Ag, namely the dissolution of Ag^+. Therefore, the impact of ionic solutions of Ag^+ on algae movement was also evaluated (Fig. 2b and c). The Ag^+ gradient was generated from 10 laminar streams of the $AgNO_3$ solution entering the microfluidics device, with minimal turbidity and little opportunity for diffusion of Ag^+ across the gradient during the measurement period. The Ag^+ dissolution in a suspension of 6×10^8 *n*Ag particles/mL was determined to be ~5 nM (Table 1). Preliminary experiments (data not shown) indicated that algae did not exhibit a response that was different from the control ($NaNO_3$ vs. $NaNO_3$ condition, Fig. S6) when it was exposed to $AgNO_3$ concentrations as high as 100 nM. The change in swimming direction of *C. reinhardtii* exposed to a gradient having a maximum concentration of 1 µM $AgNO_3$ was significant ($F_{1, 13} = 30.11$, $p < 10^{-3}$, Fig. 2b). However, no change in swimming direction was observed for *C. reinhardtii* that encountered a gradient with a maximum concentration of 10 µM $AgNO_3$ ($F_{1, 13} = 0.04$, p = n.a., Fig. 2c). This suggests that most *C. reinhardtii* did not detect areas across the gradient ≤10 µM $AgNO_3$ that would reduce their exposure to Ag^+. This is possible, as the Ag^+

concentration near the middle of the microfluidics device would have exceeded the threshold of Ag^+ concentrations known to cause cellular stress (~0.1 to 3 μM Ag^+)[16-19] over exposure times of 15 min to 24 h. High Ag^+ concentrations in the middle of the microfluidics device presents such an abundance of Ag^+ ions that the algae may have been unable to determine an alternative direction where they could move to avoid the toxic Ag^+ environment.

C. reinhardtii significantly changes direction away from nAg at 10^8 particles/mL, but not nAu or nSPL

The swimming direction of *C. reinhardtii* was not affected by exposure to a gradient with a maximum concentration of 6×10^7 particles/mL of *n*Ag, but there was a significant change in the swimming direction towards the buffer solution and away from *n*Ag at exposure levels of 6×10^8, 6×10^9 and 6×10^{10} particles/mL (Fig. 3a-d). The 6×10^8 *n*Ag particles/mL condition contains ~0.5 μM total Ag. However, with dissolution considered (Fig. S1), the Ag^+ content is estimated to be ~5 nM (Table 1), considerably less than the lowest concentration of Ag^+ tested. Slopes of the regression lines describing the observed density of *C. reinhardtii* exposed to 1 μM $AgNO_3$ and the 6×10^8 *n*Ag particles/mL were also significantly different ($t_{26} = 4.04$, $p < 10^{-3}$), indicating the algae found *n*Ag significantly more repellent than the Ag^+.

In contrast, exposure to *n*Au particles did not change the movement of *C. reinhardtii* (Fig. 4). This was unexpected because *n*Ag and *n*Au have similar size, charge, and density, as well as the same coating material and manufacturer. Since *C. reinhardtii* did not change their swimming direction to avoid contact with *n*Au, but altered their direction significantly to avoid *n*Ag when a similar number of particles (6×10^8 or 6×10^9 particles/mL) were present, we deduce that the aversive swimming response to *n*Ag was due to its chemical properties (i.e., dissolved Ag^+ around

the particle) rather than its physical properties (e.g., size, charge, density) (Note: it was not possible to conduct experiments with *n*Au at 6×10^{10} particles/mL or higher concentrations due to the lower concentration of the commercial stock suspension).

A sulfated polystyrene latex particle (*n*SPL) (commercially available at a higher stock concentration) was selected as an additional model ENP. The *n*SPL differs from the *n*Ag and *n*Au because it is uncoated, has a lower density, is not a metal, does not release ions and is less than half the diameter of the other ENPs (22 nm vs. 50 nm). It is considered non-toxic, and we believed an appropriate model ENP to evaluate responses of *C. reinhardtii* to nano-sized objects in the microfluidics device. Algal movement in the presence of *n*SPL was similar to swimming behavior in the presence of a comparable number of *n*Au particles (compare Fig. 4b and Fig 5a). Comparing *n*SPL to *n*Au in the 10^9 conditions (Fig. 4b and Fig 5a), although the *n*SPL is a lower nominal concentration (3 vs. 6 coefficent) it was closer to significance ($p = 0.08$ *n*SPL vs. 0.75 *n*Au; Table S2). When the SSA of ENP were considered, the comparable concentrations of *n*Au (6×10^8 particles) and *n*SPL (3×10^9 particles) induced non-significant responses in *C. reinhardtii* movement (Fig. 4a and 5a). There was no significant avoidance of *n*Au at 6×10^9 particles/mL, but the algae did avoid *n*SPL at a comparable concentration of 3×10^{10} particles/mL and higher (Fig. 4b and 5b). This may indicate that increasing the concentrations of non-toxic nanoparticles can induce avoidance behaviour through an undescribed mechanism, or that the *n*SPL possesses some element of subacute toxicity that is not yet understood.

Discussion

Survival of motile organisms in polluted environments is strongly linked to their physical responses. The ability to detect and move away from deleterious contaminants, thereby reducing

the exposure time and concentration of toxic substances encountered, can greatly alleviate the potential toxicity to individual organisms. This investigation produced a set of novel observations captured from videos describing the swimming behavior of individual algae within a microfluidics device during an acute exposure to ENPs and $AgNO_3$. The unique finding of this study was that *C. reinhardtii* significantly avoided *n*Ag, but not *n*Au, at exposure gradients with maximum concentrations of 6×10^8 or 6×10^9 particles/mL. Additionally, *C. reinhardtii* avoided Ag^+ in gradients with a maximum concentration of 1 µM (a concentration with similar total metal content by mass compared to 6×10^8 *n*Ag and *n*Au). These results provide compelling evidence that *n*Ag posed a detectable threat to *C. reinhardtii*, such that $\geq10^8$ particles/mL of the *n*Ag particles induced an immediate change in swimming direction. However, this was not due to the size, mass or density of the *n*Ag particles, as the algae did not avoid *n*Au. Rather, we postulate that *n*Ag particles are avoided because the colloidal *n*Ag is surrounded locally by toxic Ag^+. The potential toxic effects arising from the dissolved Ag^+ located on and/or around the colloidal *n*Ag must therefore relay enough information to the organism's sensory apparatus that the particle and surrounding ions are detected. Consequently, the algae alters its swimming direction to avoid multiple, or further, contacts with *n*Ag (and the cell stress associated with the Ag^+ found there).

It is worth noting that compared to a $AgNO_3$ solution, the silver ions released from the *n*Ag are most likely localized around the particles and therefore would be non-uniformly distributed in the microfluidics device. Additionally, toxicity is traditionally measured using doubling concentrations,[33] but in this case, were measured over orders of magnitude to make an assessment of the 'particle'-'algae'-'exposure area size' interaction practical. The inconsistent response to Ag^+ at 1 µM (significant) and 10 µM (not significant), may indicate that we are above a threshold and the algae are unable to determine the appropriate direction for avoidance. Below 0.1 µM Ag^+,

algae may not face enough of a toxic threat to change their overall swimming direction. There was no visible evidence of toxicity (i.e., cessation of flagella, change in cell morphology, etc.) from exposure to *n*Ag or $AgNO_3$ over the course of this study (max. expected exposure ~32 s); in agreement with the onset of Ag-*C. reinhardtii* toxicity described previously (~15 min to 8 h, depending on the measured end point).[16-19, 29]

The microfluidics device used in this study permitted observation of individual organisms interacting with ENPs in real time, giving an overview of instantaneous biological responses in the population. Due to the novelty of this work (there are no directly comparable studies), it is helpful to consider some mathematical cases. The microfluidic device can be represented as an exposure chamber composed of ten distinct 100 µm wide streams of ENPs, each representing a concentration that together span approximately an order of magnitude (Supplementary Fig. S7). The highest concentration of ENPs is present at the edge of the microfluidics device, and rapidly decreases to a particle-free background solution at the opposite side of the chamber.

At an inlet concentration of 6×10^8 particles/mL, the theoretical midpoint concentration is between 1.9 and 4.5×10^8 *n*Ag/mL. If an alga enters the device and swims toward the low concentration side (about ~1×10^8 *n*Ag/mL in this case) there would be approximately 2800 nanoparticles in that stream. Given the volume of the stream, it could contain 1.7×10^5 algae. Thus, the alga has a ~1.6 % chance of encountering a *n*Ag particle. If an alga were to swim into the stream containing the highest concentration (~6×10^8 *n*Ag/mL in this case) of *n*Ag, it would then have an 9.9 % chance of contacting a *n*Ag particle. We can determine the likelihood that an alga would encounter a *n*Ag particle during its residence time in the device using the equation of the general form given in Eq. 1:

$$1 - (1 - P)^N \qquad (1)$$

where, *P* is the probability of an alga encountering a particle and *N* is the number of potential encounters, or the proportional length of the device (i.e. device length divided by alga length). The results of these calculations for a range of *n*Ag concentrations are presented in Table 1. These cases are based on the following assumptions: *i*) that the algae move relative to the liquid, *ii*) that the particles are not moving and spaced an equal distance apart, and *iii*) the algae completely fill their space, i.e., a rectangular shaped unit with volume equal to 500 μm^3.

In Table 1, the general form of Eq. 1 is solved for length (in algae body lengths) that a microfluidics device would need to be for algae to encounter at least one particle (i.e., the limit of Eq. 1 as *P* approaches 1) at each *n*Ag concentration. In the device used herein (14 mm, or 1400 algae in length), at concentrations of 6×10^7 *n*Ag particles/mL or greater, we estimated that algae have a 100 % likelihood of contacting at least one nanoparticle before they reach the outlet. This agrees with our observation of significant swimming avoidance at and above inlet concentrations of 6×10^8 particles/mL *n*Ag, in which the midpoint and low concentration side of the device would have been on the order of 10^7.

Algae also had 100 % probability of encountering ENPs in the streams containing 10^8 or 10^9 particles/mL of *n*Au and *n*SPL in our experiment, but did not alter their swimming direction at these exposure levels. Only a high inlet concentration of 3×10^{10} *n*SPL/mL resulted in a significant change in swimming direction. Algae were essentially pummelled by particles in the stream containing 3×10^{10} particles/mL, so the observation could be interpreted as avoidance behavior. Mechanotransduction – a sensory mechanism demonstrated in *C. reinhardtii* previously[26] – may be related to the resulting movement towards the buffer solution and away from potentially hitting numerous tiny particles in the stream containing 3×10^{10} *n*SPL.

Avoidance of ENPs could also be induced by their physical properties that can lead to repulsive electrostatic or hydrophobic interactions, or through an unconsidered factor such as trace left-over production reagents or stabilizers. The activation of general stress-response mechanisms implicated previously with silver or other metal toxicity, such as ROS-detoxifying enzymes like prenyllipids, or the up- or down-regulation of metabolic pathways[34-36] could be involved in the avoidance response. Comparing these stress-response systems to the activation of systems involved in mechanotransduction (e.g., receptor-like kinases, or mechanosensitive channels such as MscS)[37-39] could be areas of future research to further elucidate the mechanisms behind the avoidance of non-toxic particles at concentrations with a high collision likelihood.

The video footage of algae swimming in this study was examined carefully, and there were more instances where algae seemed to collide with *n*Ag than the calculated percentages would indicate. A contact between algae and *n*Ag is difficult to confirm by visual observations because of the parallax of the microscope and the disproportional scattering of light by *n*Ag. This could give the appearance of contact between an algae and *n*Ag that did not occur, either because the two objects were in different planes of the fluid, or the particle was much smaller than it appeared.

Conclusion

This study employed a novel, individual organism-based approach to assess the avoidance response of *C. reinhardtii* to *n*Ag. A microfluidics device offers a realistic environment where algae were exposed to variable toxicant concentrations. Individual algae demonstrated their ability to swim away from known toxicants *n*Ag and Ag^+, but showed greater avoidance of *n*Ag despite a much lower measured concentration of dissolved Ag^+ in *n*Ag suspensions than in tested $AgNO_3$ solutions. We contend that the avoidance response observed is a result of the general cell stress experienced by algae in the presence of both forms of silver (i.e., Ag^+ and *n*Ag). Furthermore, we did not observe avoidance of a comparable ENP, *n*Au, at similar concentrations. However, adverse responses to another non-threatening material, *n*SPL, were observed at concentrations two orders of magnitude greater than *n*Ag. Therefore, we posit that non-toxic particles may be able to elicit a physical avoidance response through mechanotransduction, although further studies are needed in this area. Further investigation is also needed regarding the role of different types of coatings in potentially shielding ENPs from detection by organisms in the environment. Additional studies involving other particles that cause chemical toxicity and/or physical stimulation of algae would aid in determining the generalizability of these findings. Direct measurement of contact between algae-ENPs could help unravel the mechanisms, whether chemical or physical, that *C. reinhardtii* rely upon to avoid *n*Ag and/or Ag^+.

References

(1) Keller, A. A., McFerran, S., Lazarova, A. & Suh, S. Global life-cycle releases of engineered nanomaterials. *J. Nanopart. Res.* **15 (6),** 1692-1694 (2013).

(2) Rai, M., Yadav, A. & Gade, A. Silver nanoparticles as a new generation of antimicrobials. *Biotechnol. Adv.* **27 (1),** 7-83 (2009).

(3) Benn, T. M. & Westerhoff, P. Nanoparticle silver released into water from commercially available sock fabrics. *Environ. Sci. Technol.* **42 (11)**, 4133-4139 (2008).

(4) Lowry, G. V. & Wiesner, M. R. Environmental considerations: Occurrences and fate of nanomaterials in the environment in *Nanotoxicology: Characterization, Dosing, and Health Effects* (eds. Monteiro-Riviere, N. & Tran, C. L.) 369-390 (Infoma Health Care USA, 2007).

(5) Cornelis, G. Fate descriptors for engineered nanoparticles: the good, the bad, and the ugly. *Environ. Sci. Nano* **2 (1),** 19-26 (2015).

(6) Troester, M., Brauch, H. J. & Hofmann, T. Vulnerability of drinking water supplies to engineered nanoparticles. *Wat. Res.* **96,** 255-279 (2016).

(7) Bondarenko, O. *et al.* Toxicity of Ag, CuO and ZnO nanoparticles to selected environmentally relevant test organisms and mammalian cells in vitro: a critical review. *Arch. Toxicol.* **87 (7),** 1181-1200 (2013).

(8) Ivask, A. *et al.* Size-dependent toxicity of silver nanoparticles to bacteria, yeast, algae, crustaceans and mammalian cells in vitro. *PLoS One* **9 (7),** e102108 (2014).

(9) Dorobantu, L.S. *et al.* Toxicity of silver nanoparticles against bacteria, yeast, and algae. *J. Nanopart. Res.* **17 (4),** 1-13 (2015).

(10) Zhang, C., Hu, Z. & Deng, B. Silver nanoparticles in aquatic environments: Physiochemical behavior and antimicrobial mechanisms. *Wat. Res.* **88,** 403-427 (2016).

(11) Morones, J.R. *et al.* The bactericidal effect of silver nanoparticles. *Nanotechnology*, **16 (10),** 2346 (2005).

(12) Foldbjerg, R. & Autrup, H. 2013. Mechanisms of silver nanoparticle toxicity. *Arch. Basic Appl. Med.* **1 (1),** 5-15 (2013).

(13) Reidy, B., Haase, A., Luch, A., Dawson, K.A. & Lynch, I. Mechanisms of silver nanoparticle release, transformation and toxicity: a critical review of current knowledge and recommendations for future studies and applications. *Materials* **6 (6),** 2295-2350 (2013).

(14) Xiu, Z.M., Zhang, Q.B., Puppala, H.L., Colvin, V.L. & Alvarez, P.J. Negligible particle-specific antibacterial activity of silver nanoparticles. *Nano Lett.* **12 (8),** 4271-4275 (2012).

(15) Shrager, J. *et al. Chlamydomonas reinhardtii genome* project. A guide to the generation and use of the cDNA information. *Plant Physiol.* **131 (2),** 401-408 (2003).

(16) Moreno-Garrido, I., Pérez, S. & Blasco, J. Toxicity of silver and gold nanoparticles on marine microalgae. *Mar. Environ. Res.* **111,** 60-73 (2015).

(17) Lee, D.Y., Fortin, C. & Campbell, P.G. Contrasting effects of chloride on the toxicity of silver to two green algae, *Pseudokirchneriella subcapitata* and *Chlamydomonas reinhardtii*. *Aquat. Toxicol.* **75 (2),** 127-135 (2005).

(18) Navarro, E. *et al.* Toxicity of silver nanoparticles to *Chlamydomonas reinhardtii*. *Environ. Sci. Technol.* **42 (23),** 8959-8964 (2008).

(19) Navarro, E., Wagner, B., Odzak, N., Sigg, L. & Behra, R. Effects of differently coated silver nanoparticles on the photosynthesis of *Chlamydomonas reinhardtii*. *Environ. Sci. Technol.* **49 (13),** 8041-8047 (2015).

(20) Pillai, S. *et al.* Linking toxicity and adaptive responses across the transcriptome, proteome, and phenotype of *Chlamydomonas reinhardtii* exposed to silver. *Proc. Natl. Acad. Sci.* **111 (9),** 3490-3495 (2014).
(21) Sjoblad, R.D. & Frederikse, P.H. Chemotactic responses of *Chlamydomonas reinhardtii*. *Mol. Cell. Biol.* **1 (12),** 1057-1060 (1981).
(22) Govorunova, E.G. & Sineshchekov, O.A. Chemotaxis in the green flagellate alga Chlamydomonas. *Biochemistry* **70 (7),** 717-725 (2005).
(23) Stavis, R.L. & Hirschberg, R. Phototaxis in *Chlamydomonas reinhardtii*. *J. Cell Biol.* **59 (2),** 367-377 (1973).
(24) Sineshchekov, O.A., Jung, K.H. & Spudich, J.L. Two rhodopsins mediate phototaxis to low-and high-intensity light in *Chlamydomonas reinhardtii*. *Proc. Natl. Acad. Sci.* **99 (13),** 8689-8694 (2002).
(25) Govorunova, E.G., Jung, K.H., Sineshchekov, O.A. & Spudich, J.L. Chlamydomonas sensory rhodopsins A and B: cellular content and role in photophobic responses. *Biophys. J.* **86 (4),** 2342-2349 (2004).
(26) Min, S.K., Yoon, G.H., Joo, J.H., Sim, S.J. & Shin, H.S. Mechanosensitive physiology of *Chlamydomonas reinhardtii* under direct membrane distortion. *Sci. Rep.* **4,** 4675 (2014).
(27) Englert, D. L., Manson, M. D. & Jayaraman, A. Flow-based microfluidic device for quantifying bacterial chemotaxis in stable, competing gradients. *Appl. Environ. Microbiol.* **75 (13),** 4557-4564 (2009).
(28) Englert, D. L., Manson, M. D. & Jayaraman, A. Investigation of bacterial chemotaxis in flow-based microfluidic devices. *Nat. Protoc.* **5 (5),** 864-872 (2010).
(29) Simon, D. F. *et al.* Transcriptome sequencing (RNA-seq) analysis of the effects of metal nanoparticle exposure on the transcriptome of *Chlamydomonas reinhardtii*. *Appl. Environ. Microbiol.* **79 (16),** 4774-4785 (2013).
(30) Lockwood, A. P. M. "Ringer", solutions and some notes on the physiological basis of their ionic composition. *Comp. Biochem. Phys.* **2 (4),** 241-289 (1961).
(31) Stocker, R. & Durham, W.M. Tumbling for stealth?. *Science* **325 (5939),** 400-402. (2009).
(32) Polin, M., Tuval, I., Drescher, K., Gollub, J.P. & Goldstein, R.E. Chlamydomonas swims with two "gears" in a eukaryotic version of run-and-tumble locomotion. *Science* **325 (5939),** 487-490 (2009).
(33) Rand, G. M. (Ed.). *Fundamentals of aquatic toxicology: effects, environmental fate and risk assessment.* CRC Press. Chicago. (1995)
(34) Nowicka, B., Pluciński, B., Kuczyńska, P. & Kruk, J. Prenyllipid antioxidants participate in response to acute stress induced by heavy metals in green microalga *Chlamydomonas reinhardtii*. *Environ. Exp. Bot.* **123,** 98-107. (2016).
(35) da Costa, C. H., Perreault, F., Oukarroum, A., Melegari, S. P., Popovic, R. & Matias, W. G. Effect of chromium oxide (III) nanoparticles on the production of reactive oxygen species and photosystem II activity in the green alga *Chlamydomonas reinhardtii*. *Sci. Total Environ.* **565,** 951-960. (2016).
(36) Beauvais-Flück, R., Slaveykova, V.I. & Cosio, C. Transcriptomic and Physiological Responses of the Green Microalga Chlamydomonas reinhardtii during Short-Term Exposure to Subnanomolar Methylmercury Concentrations. *Environ. Sci. Technol.* **50 (13),** 7126-7134 (2016).
(37) Haswell, E. S. MscS-like proteins in plants. *Curr. Top. Membr.* **58,** 329-359. (2007).
(38) Yoshimura, K. Stimulus Perception and Membrane Excitation in Unicellular Alga Chlamydomonas. In: *Coding and Decoding of Calcium Signals in Plants.* pp. 79-91. Springer. Berlin Heidelberg. (2011).
(39) Monshausen, G. B. & Haswell, E. S. A force of nature: molecular mechanisms of mechanoperception in plants. *J. Exp. Bot.* **64 (15),** 4663-4680. (2013).

Acknowledgements

The authors acknowledge the financial support of the Canada Research Chairs program, Natural Sciences and Engineering Research Council of Canada, Environment Canada, Vive Crop Protection, the Ministère du Développement économique, Innovation et Exportation (MDEIE), the FRQNT, the Concordia Institute for Water, Energy and Sustainable Systems for a CREATE award to MRM. The authors thank K.J. Wilkinson for providing the source *C. reinhardtti*; C. Moraes for the use of the plasma oxidizer; A. Azimzada for performing ICP-MS measurements; M. I. Deng, A. Giordano and H.Y. Seo for their assistance with video analysis; and A. Beland, A. Olsson, A. Wargenau, and N. Yousefi for helpful discussions.

Author contributions

M.M., N.L., J.W., and N.T. conceived the experiments. M.M. and N.L. conducted the experiments. M.M. analysed the experimental results. All authors contributed to writing of the manuscript.

Competing financial interests

The authors declare no competing financial interests.

Table 1. Summary of calculations of contact likelihood between algae and ENPs (molarity given for *n*Ag)**.**

[ENP] (particles/mL)	[ENP] (mg/L)	[ENP] (µM)	Dissolved Ag^+ content† (µM)	% Likelihood of ENP Encounter when $N = 1$	% Likelihood of ENP Encounter when $N = 1400$	# of algae lengths, when $p \rightarrow 1$*
1×10^6	0.001	0.01	n.d.	0.016	21	61890
6×10^6	0.005	0.05	n.d.	0.099	74	10010
1×10^7	0.010	0.1	n.d.	0.16	89	6185
6×10^7	0.05	0.50	0.002	0.99	~100	997
1×10^8	0.10	0.97	n.d.	1.6	100	615
6×10^8	0.54	5.0	0.006	9.9	100	95
1×10^9	1.0	9.7	n.d.	16	100	57
6×10^9	5.4	50	0.032	99	100	2
1×10^{10}	10	97	n.d.	164	n.d.	n.d.
6×10^{10}	54	500	3.41	990	n.d.	n.d.

† Estimated Ag^+ content based on % dissolution from ICP-MS.
N = distance in number of algae body lengths, estimated to be 10 µm.
n.d: not determined.

Figures

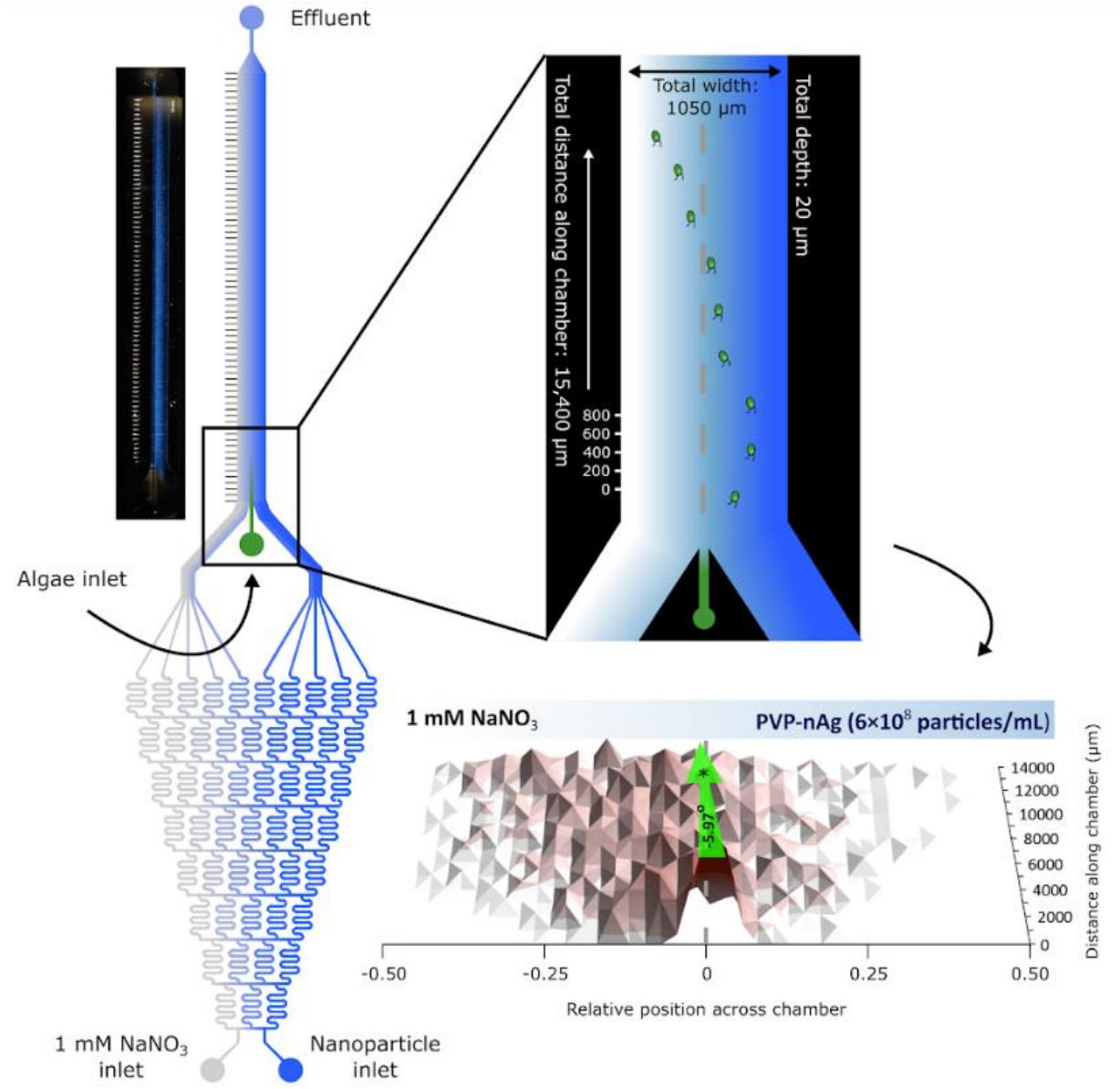

Figure 1. *Illustration of the microfluidic system for studying Chlamydomonas reinhardtii swimming behaviour when exposed to engineered nanoparticles. The exposure chamber in the microfluidic device is 20 µm × 1050 µm × 15,600 µm (h × w × l). Results are captured through videos taken every 1000 µm, starting at the rear of the microfluidic exposure chamber (14,000 µm) and moving toward the inlets (0 µm). Data are analyzed by recording the relative position within the column of the algae at each distance marker.*

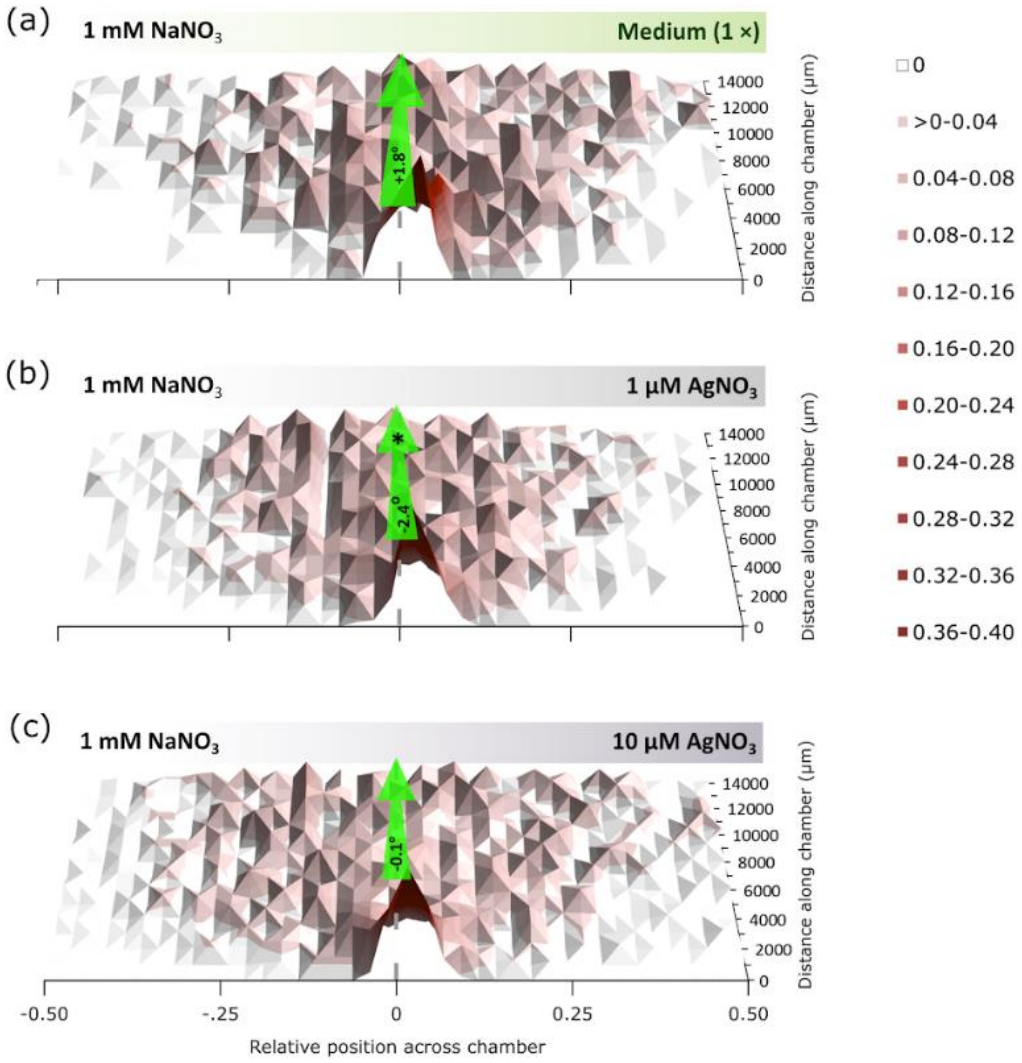

Figure 2. *3-D surface plot showing the relative number of algae observed along the microfluidic chamber at each of the 1000 µm markings for conditions filled with 1 mM $NaNO_3$ (left) and (a) algae medium (right), or solutions of (b) 1 µM, or (c) 10 µM $AgNO_3$ (right). Each colour in the legend is associated with a different proportional fraction of algae, and this is also illustrated by the height of the surface plot peaks.*

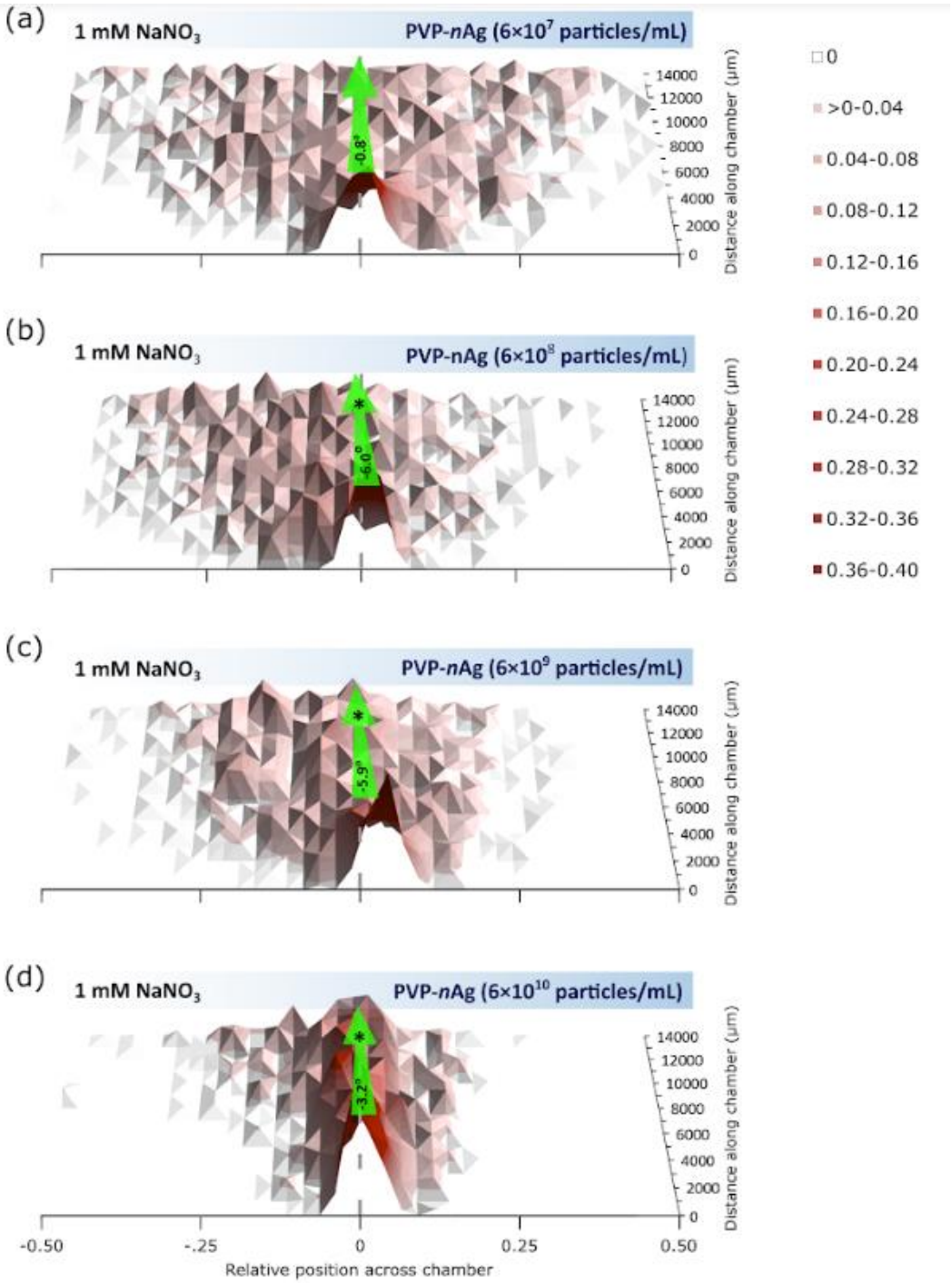

Figure 3. *3-D surface plot showing the relative number of algae observed along the microfluidic chamber at each of the 1000 µm markings for conditions filled with 1 mM $NaNO_3$ (left) and a suspension of (a) 6 × 10^7, (b) 6 × 10^8, (c) 6 × 10^9, or (d) 6 × 10^{10} PVP-nAg particles/mL (right). Each colour in the legend is associated with a different proportional fraction of algae, and this is also illustrated by the height of the surface plot peaks.*

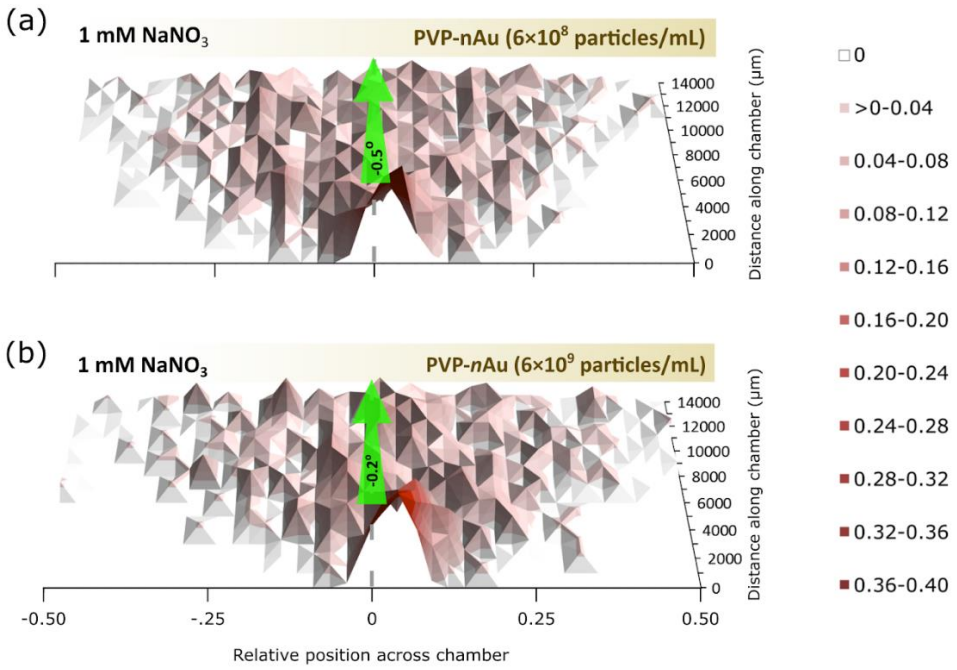

Figure 4. *3-D surface plot showing the relative number of algae observed along the microfluidic chamber at each of the 1000 µm markings for conditions filled with 1 mM $NaNO_3$ (left) and a suspension of (a) 6 × 10^8, or (b) 6 × 10^9 PVP-nAu particles/mL (right). Each colour in the legend is associated with a different proportional fraction of algae, and this is also illustrated by the height of the surface plot peaks.*

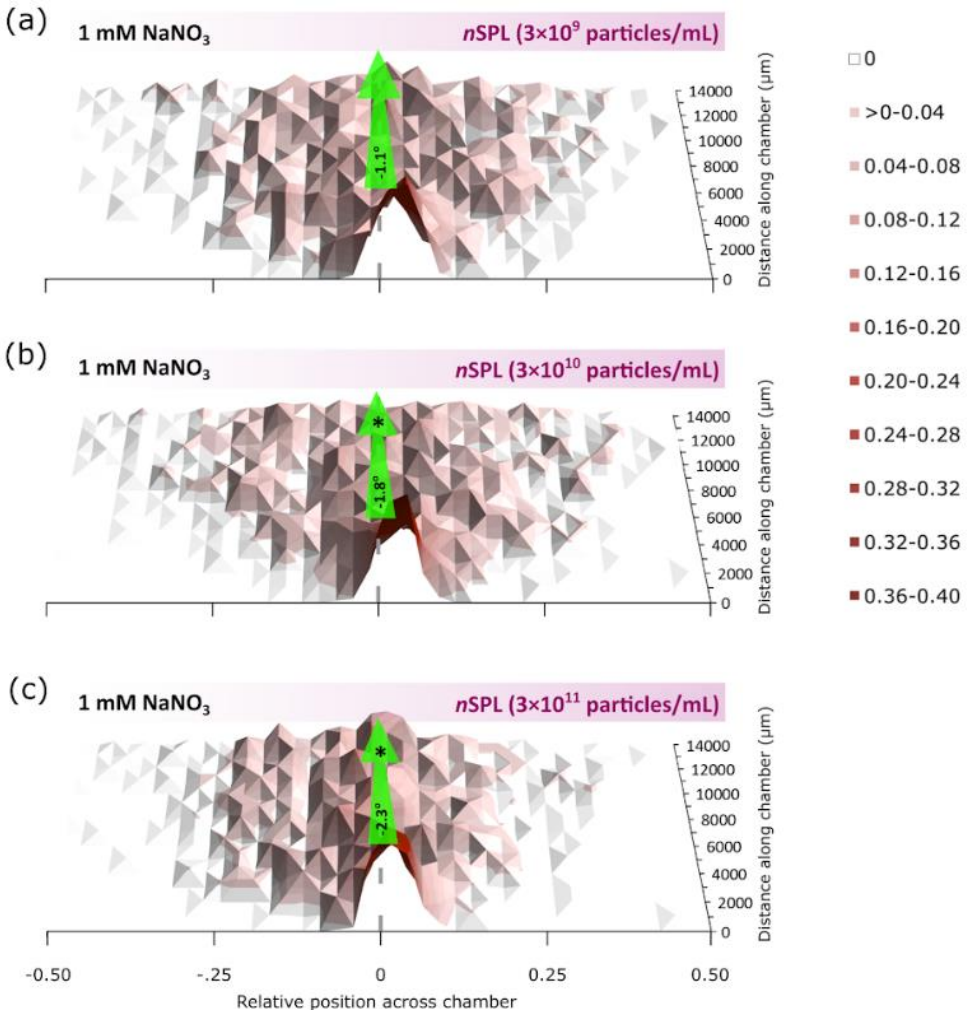

Figure 5. 3-D surface plot showing the relative number of algae observed along the microfluidic chamber at each of the 1000 µm markings for conditions filled with 1 mM $NaNO_3$ (left) and a suspension of (a) 3×10^9, (b) 3×10^{10}, or (c) 3×10^{11} *n*SPL particles/mL (right). Each colour in the legend is associated with a different proportional fraction of algae, and this is also illustrated by the height of the surface plot peaks.